



# **RADIO FREQUENCY INTERFERENCE DETECTION AND MITIGATION IN MICROWAVE RADIOMETERS**

Priscilla N. Mohammed<sup>(1, 2)</sup>

(1) NASA's Goddard Space Flight Center

(2) Morgan State University

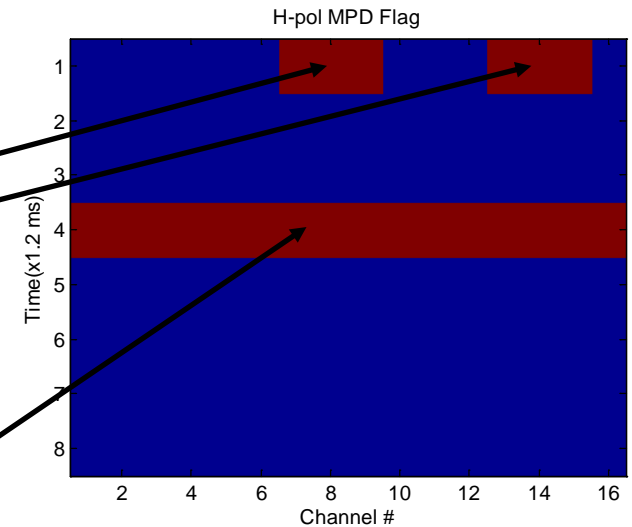
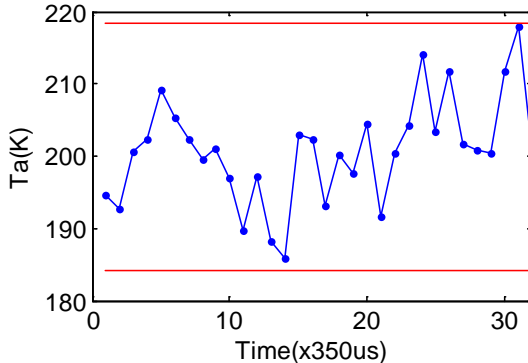
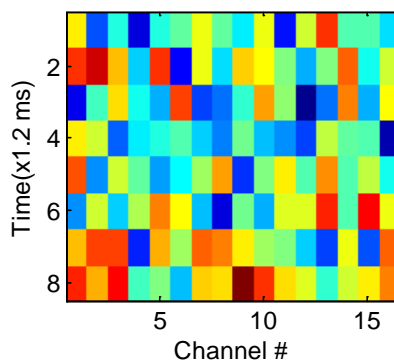
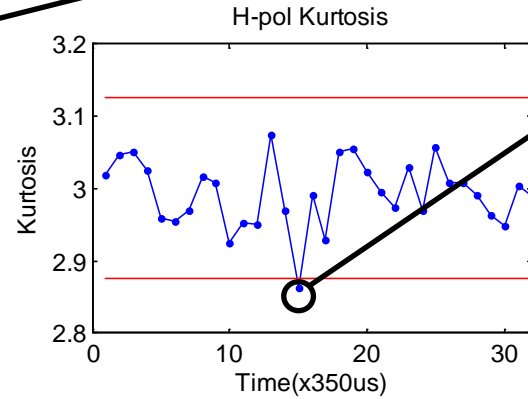
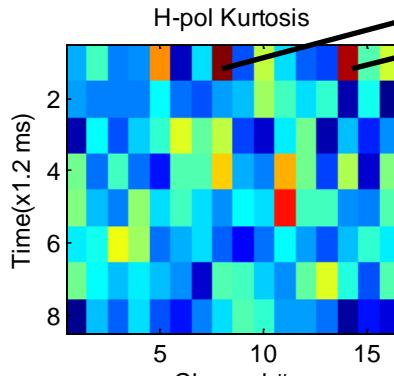


# SMAP RFI

- SMAP (Soil Moisture Active Passive) was launched by NASA January 31, 2015 to measure soil moisture of the Earth's land surface
- The SMAP radiometer operates in the L-band protected spectrum (1400-1427 MHz) that is known to be vulnerable to radio frequency interference (RFI)
  - SMOS and Aquarius provided a good indication of the RFI environment at L-band
- On orbit results show that RFI is indeed a problem
  - RFI increases brightness temperatures
  - Can lead to dry biases in soil moisture retrievals if undetected
- SMAP radiometer includes a digital backend enabling multiple RFI detection and mitigation capabilities; detection and mitigation processing performed on ground

# MAXPD

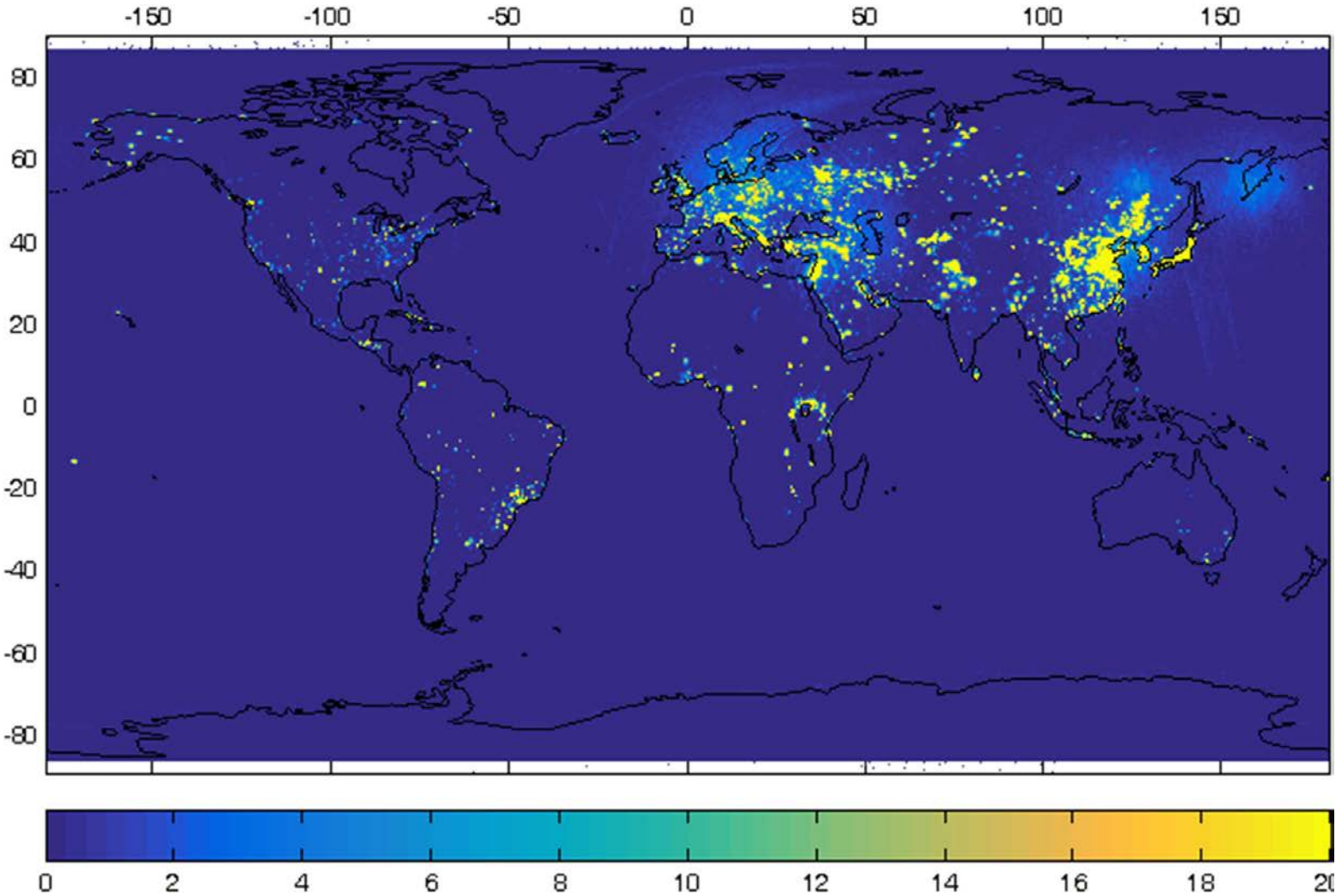
Subband detection algorithms detect and flag RFI; also flag adjacent channels: **Kurtosis, T3/T4, Cross frequency**



Time domain detectors detect and flag RFI; MPD flags corresponding time slice in subband data:  
**Pulse detector, kurtosis, T3/T4**

Drop all flagged data and average remaining clean pixels of subband data to get RFI free footprint,  $T_A$

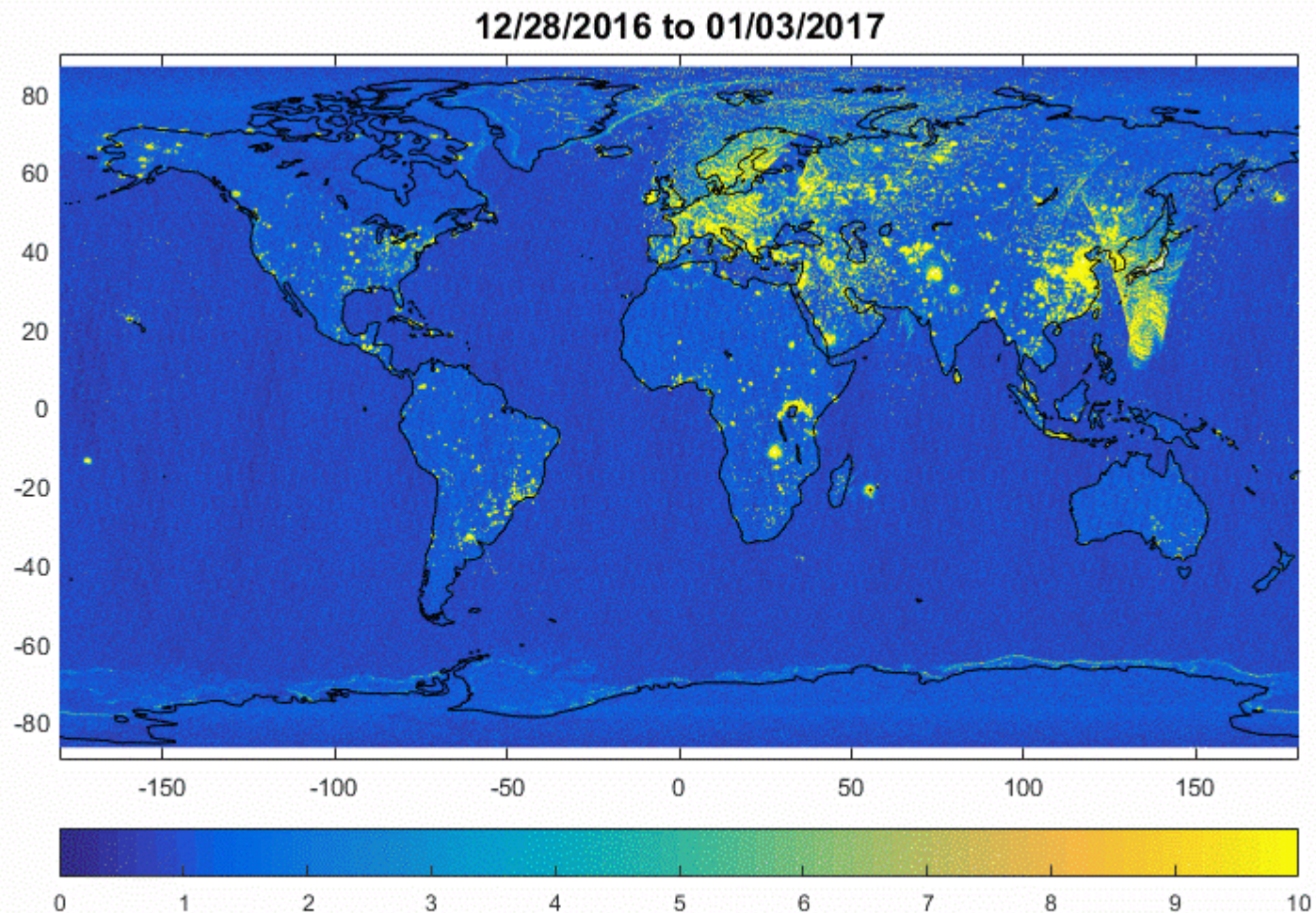
# RFI Probability Map



% of time SMAP detects RFI of 5 K or more in H-pol. April 2015 to March 2016

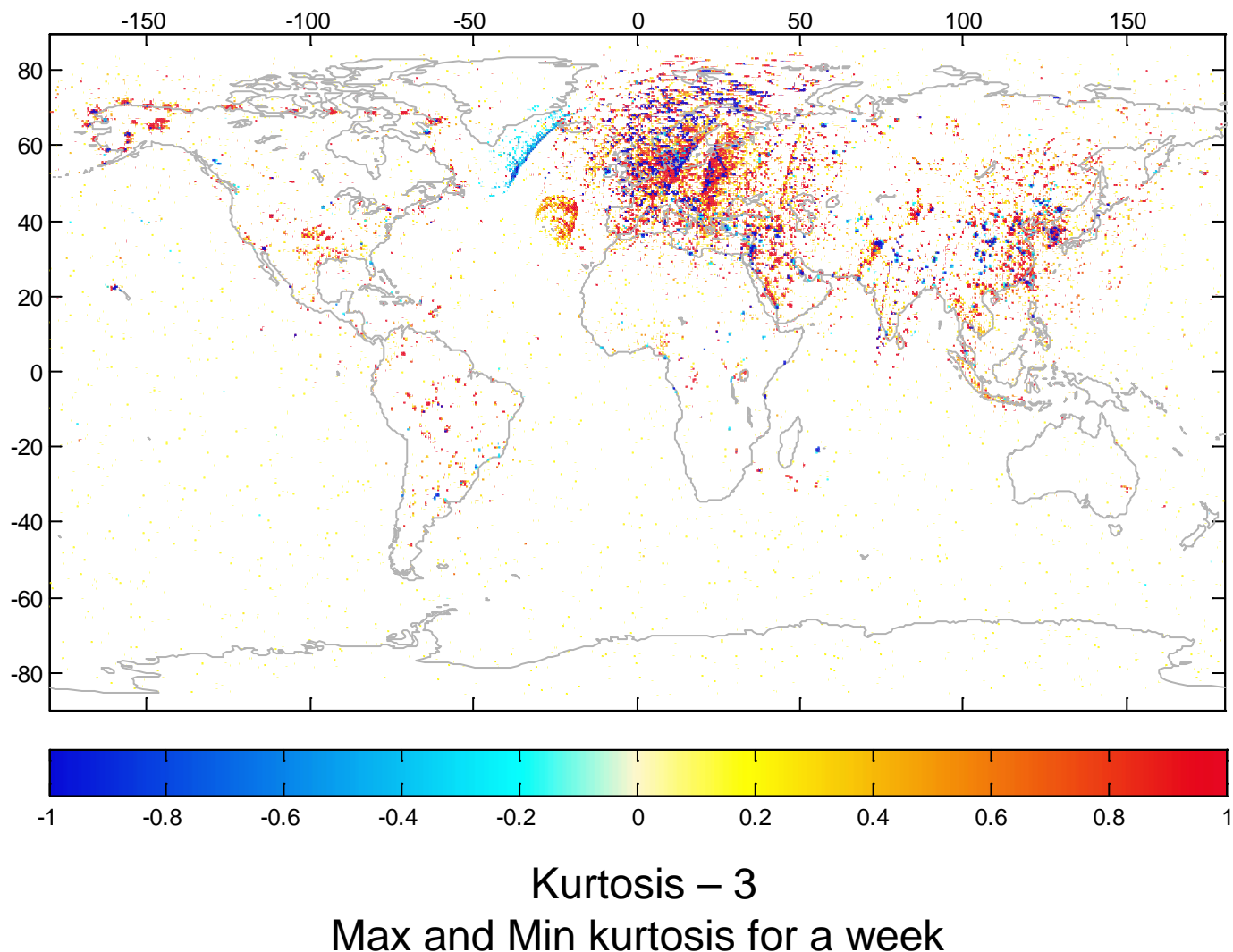
# Weekly Peak Hold RFI Maps: H-pol

- 0.25° grid
- December 2016 to May 2017
- V-pol show similar results



# Fullband Kurtosis H-pol

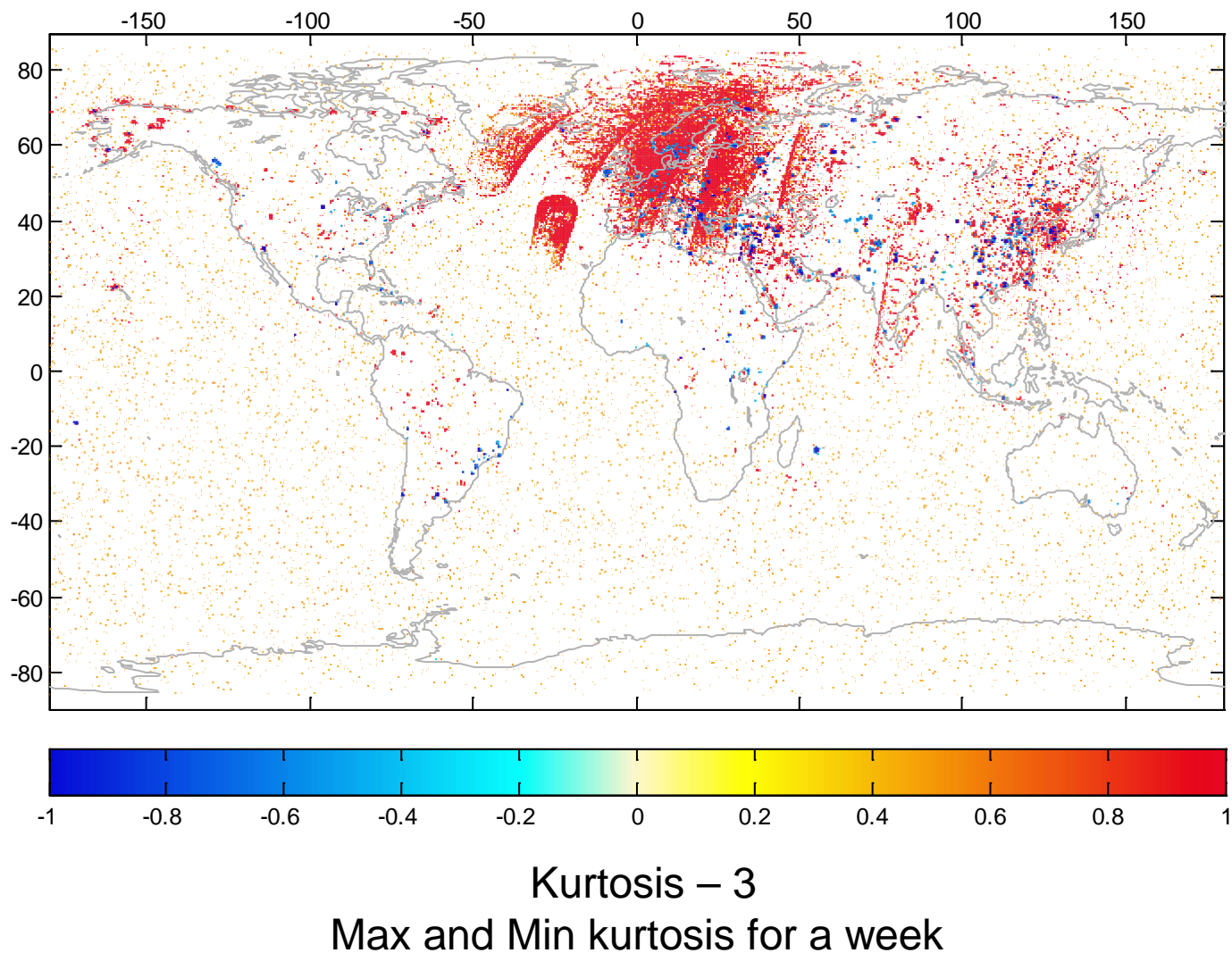
- 0.25° grid
- October
- 1-7, 2016
- V-pol  
show  
similar  
results



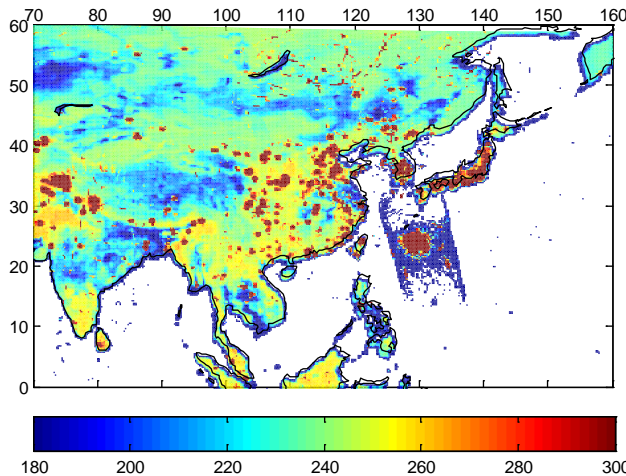


# Subband Kurtosis H-pol

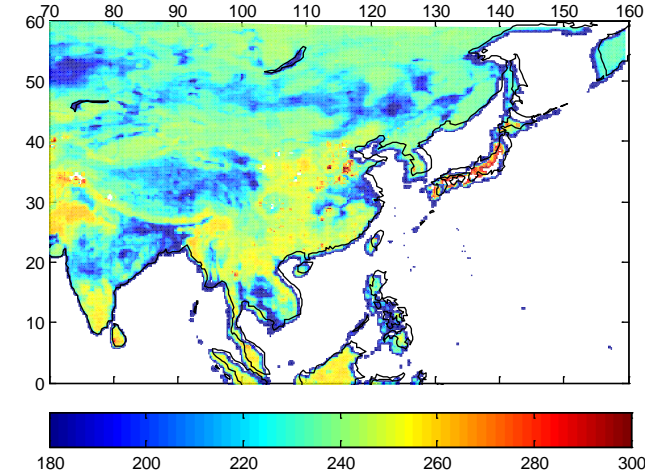
- 0.25° grid
- October
- 1-7, 2016
- V-pol
- show
- similar
- results



# TA H-pol Asia: October 1-7 2016

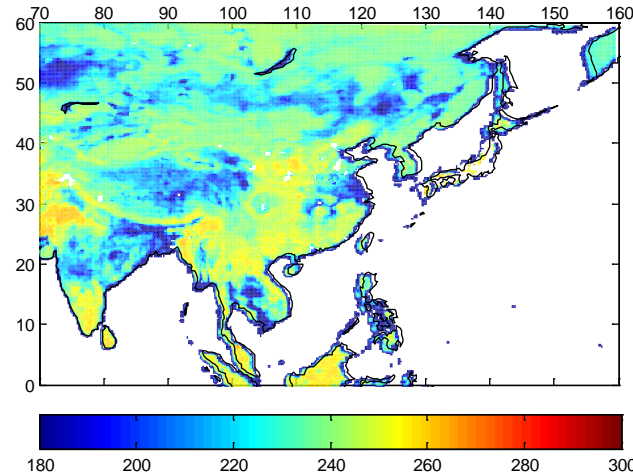


TA unfiltered



TA filtered

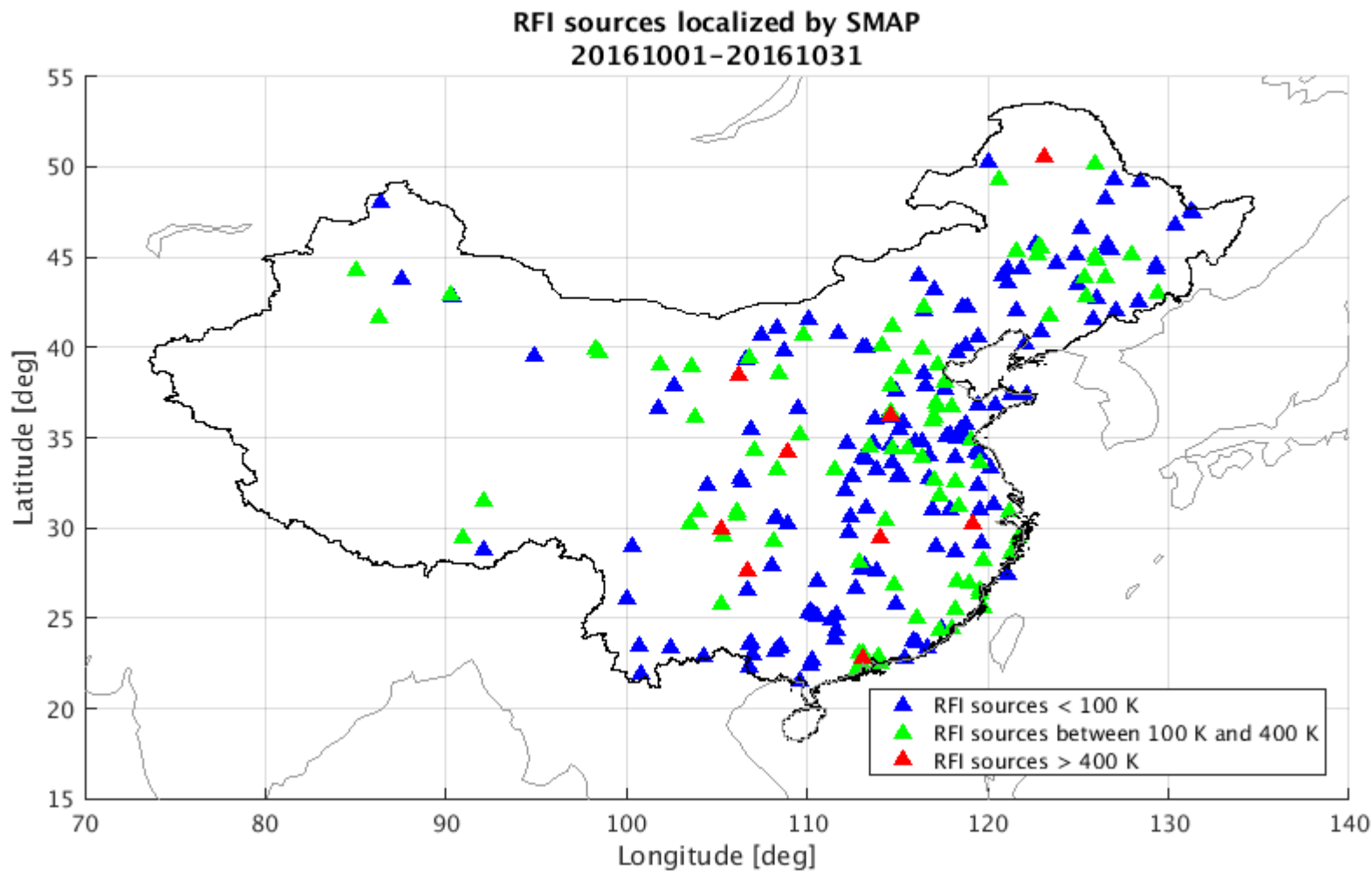
- 0.25° grid
- Peak hold,  
October 1-7,  
2016
- TA < 100 K  
omitted



TA filtered

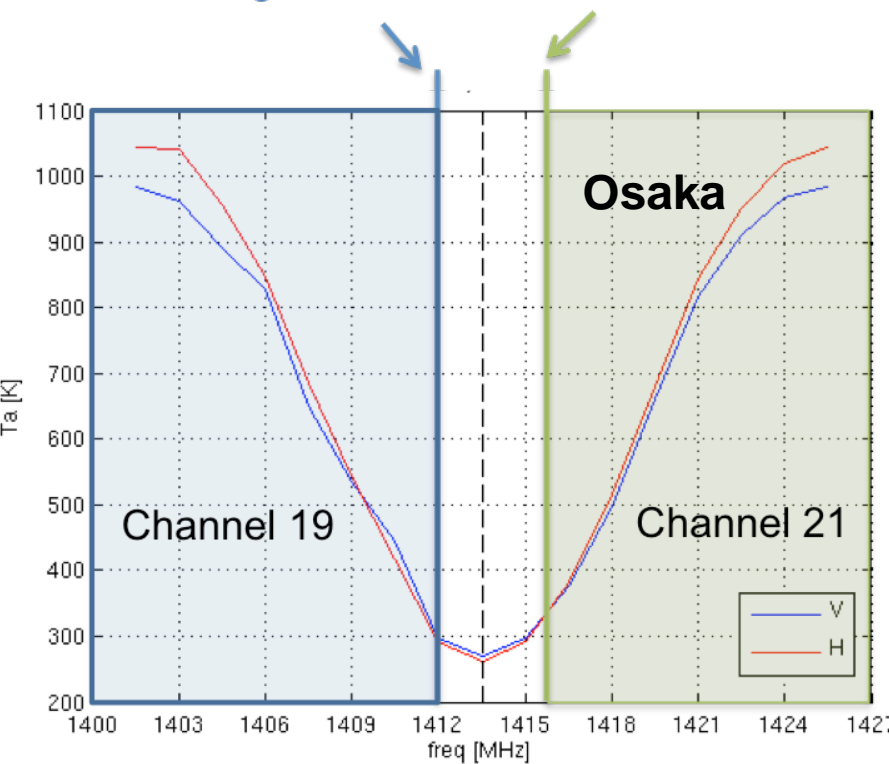
Discarding measurements  
flagged by TB quality flag;  
residual RFI could still be in  
product

# RFI Sources Localized by SMAP over China



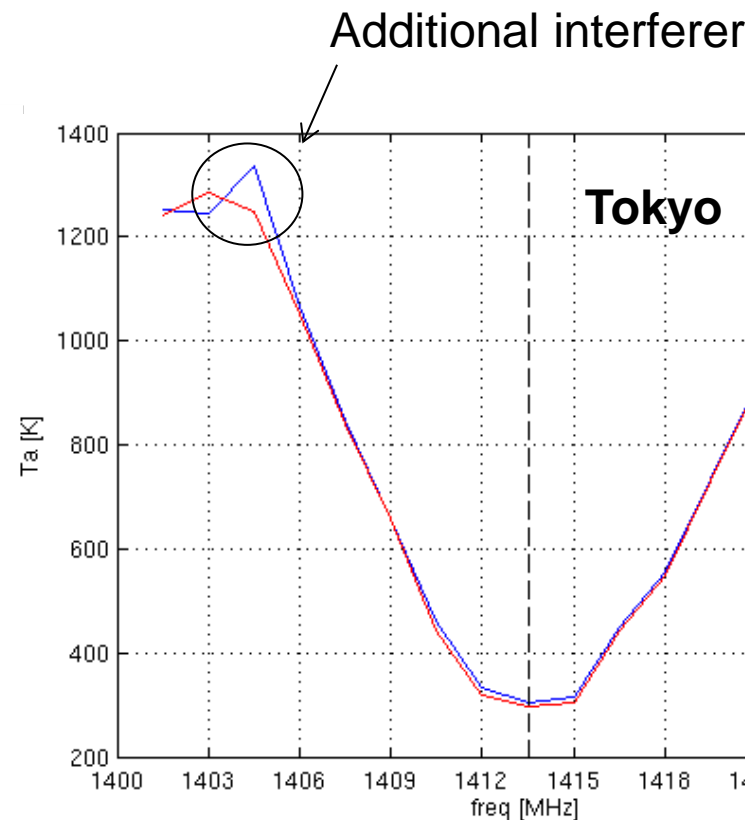
# Spectra measured by SMAP over the main Japanese cities

Stop-band of channel 19 begins here



Stop-band of channel 21 ends here

Channels 19 and 21 of the BSAT system



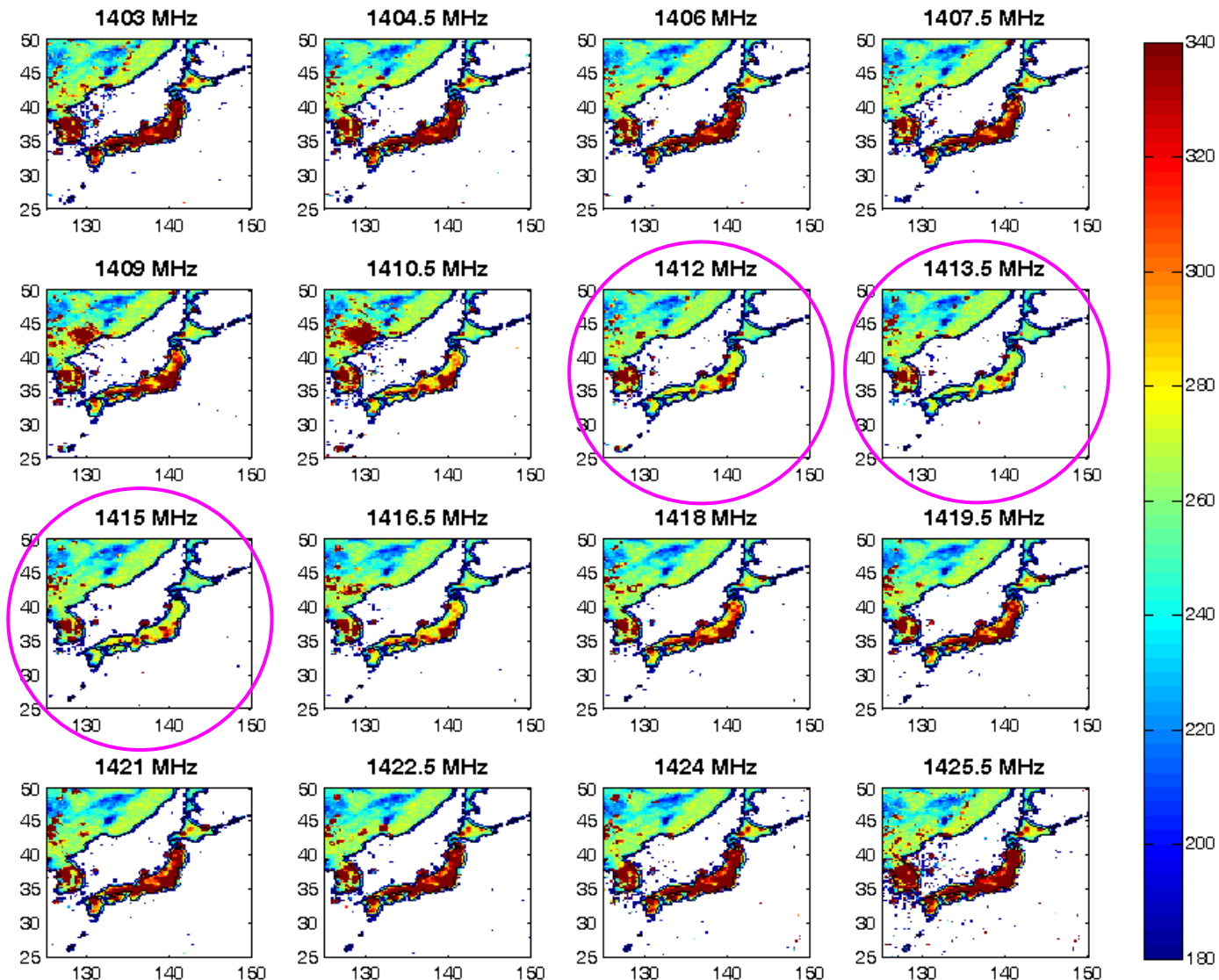
Every data point is the average of the sub-band Ta measured within a circle of 50 km radius, centered approximately at the center of the city. Similar spectra seen over **Nagoya** and **Hirosima**.



# Spectra over Japan

- 0.25° grid
- Middle channels less corrupted by RFI
- TA < 125 K omitted

TA (Kelvin)





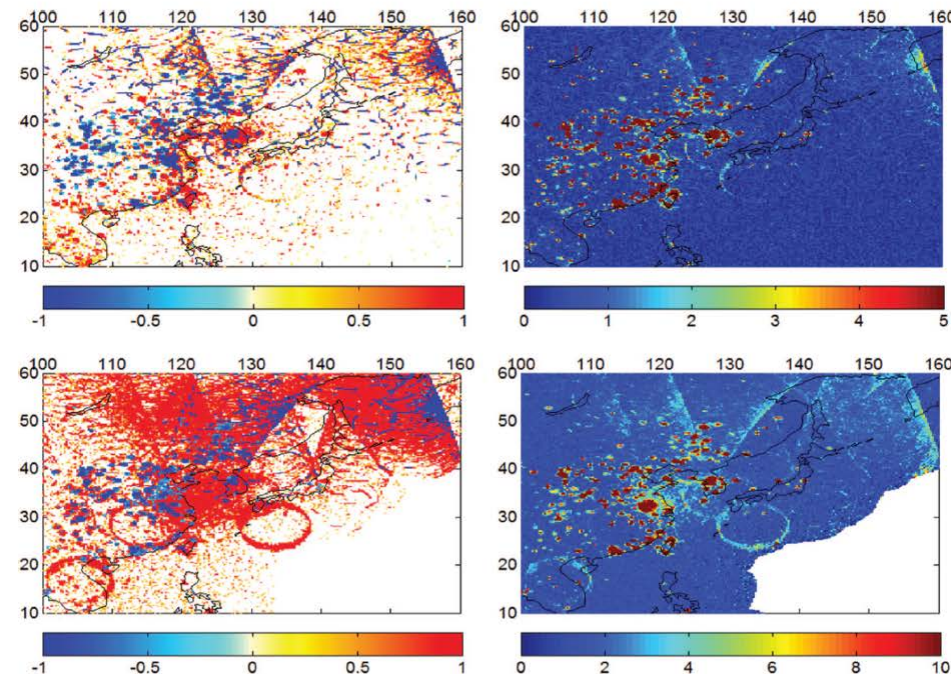
# IEEE TRANSACTIONS ON GEOSCIENCE AND REMOTE SENSING

A PUBLICATION OF THE IEEE GEOSCIENCE AND REMOTE SENSING SOCIETY



For detailed information  
on the SMAP RFI  
algorithm and results  
from the first year on  
orbit.

OCTOBER 2016 VOLUME 54 NUMBER 10 IGRSD2 (ISSN 0196-2892)



Excess kurtosis values and associated RFI detection rates in East Asia and Japan, as measured by the SMAP mission 1400–1427 MHz radiometer for the period June 3, 2015 to June 9, 2015. The top two figures are excess kurtosis values (left) and kurtosis detection rate (right) over East Asia derived from the full-bandwidth data stream. The bottom two figures show similar information obtained from the channelized data stream.

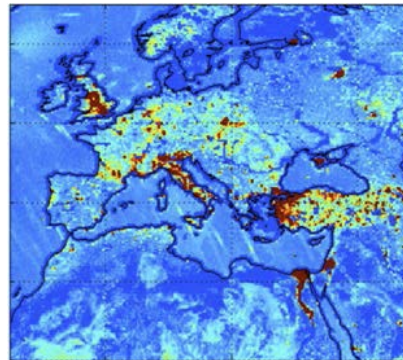


# CubeRRT: CubeSat Radiometer Radio Frequency Interference Technology Validation

PI: Joel T. Johnson, Ohio State University

## Objective

- Demonstrate wideband radio frequency interference (RFI) mitigating backend technology for future spaceborne microwave radiometers operating 6 to 40 GHz
  - Crucial to maintain US national capability for spaceborne radiometry and associated science goals
- Demonstrate successful real-time on-board RFI detection and mitigation in 1 GHz instantaneous bandwidth
- Demonstrate reliable cubesat mission operations, include tuning to Earth Exploration Satellite Service (EESS) allocated bands in the 6 to 40 GHz region



RFI sources in Europe at 10.7 GHz observed by GPM Microwave Imager



6U CubeSat layout of CubeRRT components

## Approach

- Build upon heritage of airborne and spaceborne (SMAP) digital backends for RFI mitigation in microwave radiometry
- Apply existing RFI mitigation strategies onboard spacecraft; downlink additional RFI data for assessment of onboard algorithm performance
- Integrate radiometer front end, digital backend, and wideband antenna systems into 6U CubeSat
- CSLI launch from ISS into 400 km orbit; ~ 120-300 km Earth footprint for RFI mitigation validation
- Operate for one year at 25% duty cycle to acquire adequate RFI data

## Co-Is/Partners:

C. Chen, M. Andrews, OSU; S. Misra, S. Brown, J. Kocz, R. Jarnot, JPL; D. Bradley, P. Mohammed, J. Lucey, J. Piepmeier, GSFC

## Key Milestones

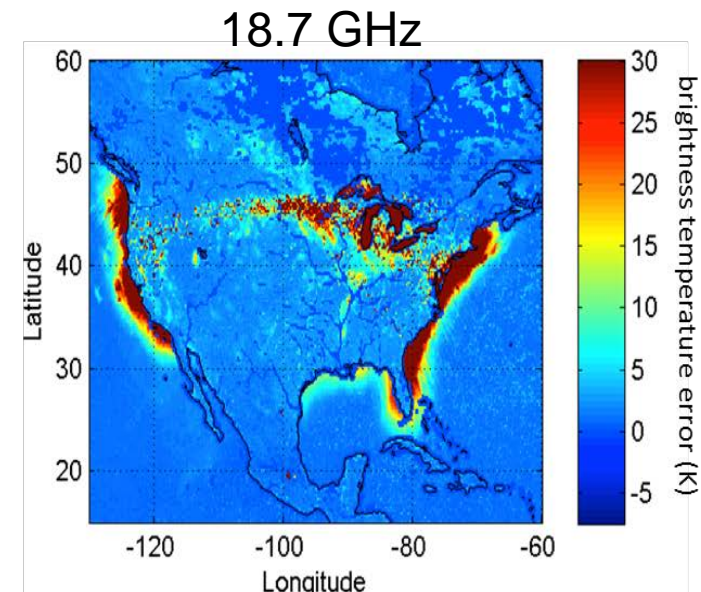
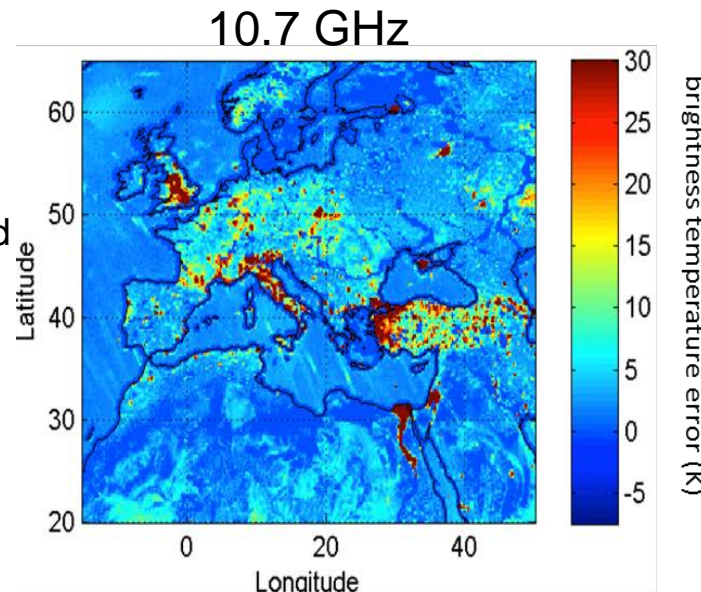
• Requirements definition and system design	03/16
• Instrument engineering model subsystem tests	4/17
• Instrument engineering model integration and test	6/17
• Instrument flight model subsystem tests	8/17
• Instrument flight model integration and test	9/17
• Spacecraft integration and test	12/17
• CubeRRT launch readiness	02/18
• On-orbit operations completion	L+12 months

$$TRL_{in} = 5 \quad TRL_{out} = 7$$

# GMI

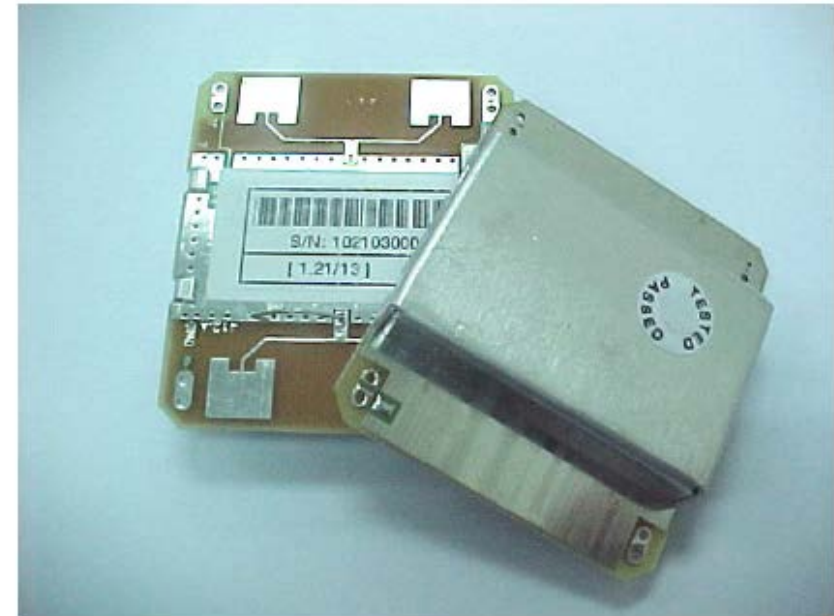
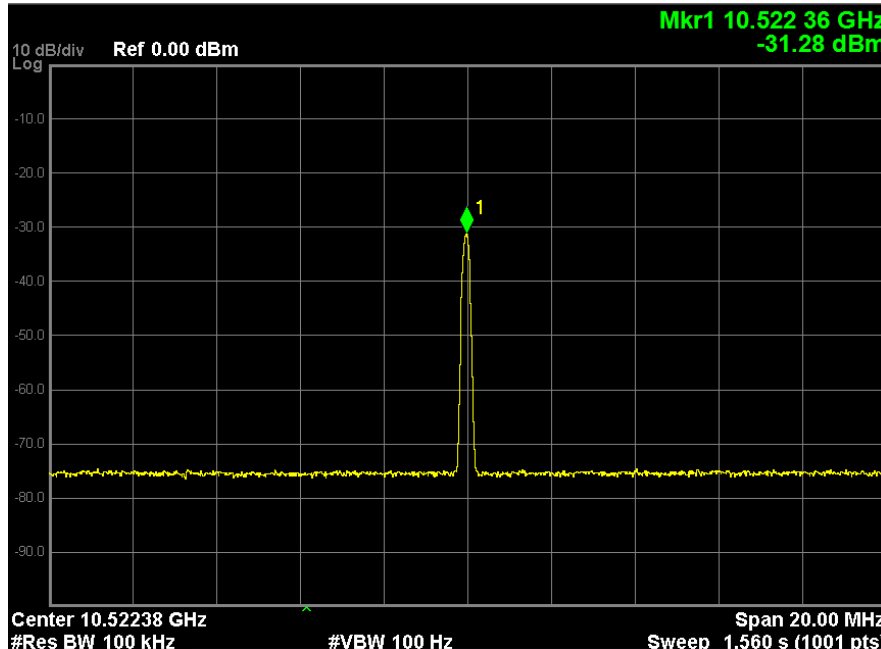
- The GMI earth-view data is contaminated by RFI in the 10 and 18 GHz channels, at both polarizations
  - 10 GHz RFI is mostly due to fixed earth emitters
  - 18 GHz low-level RFI is observed from fixed earth emitters
  - 18 GHz high-level RFI is observed from reflections off ocean and land surfaces from Geosynchronous satellites around the continental United States and Hawaii.

Picture  
courtesy  
David  
Draper and  
David  
Newell





# Motion Detector Units



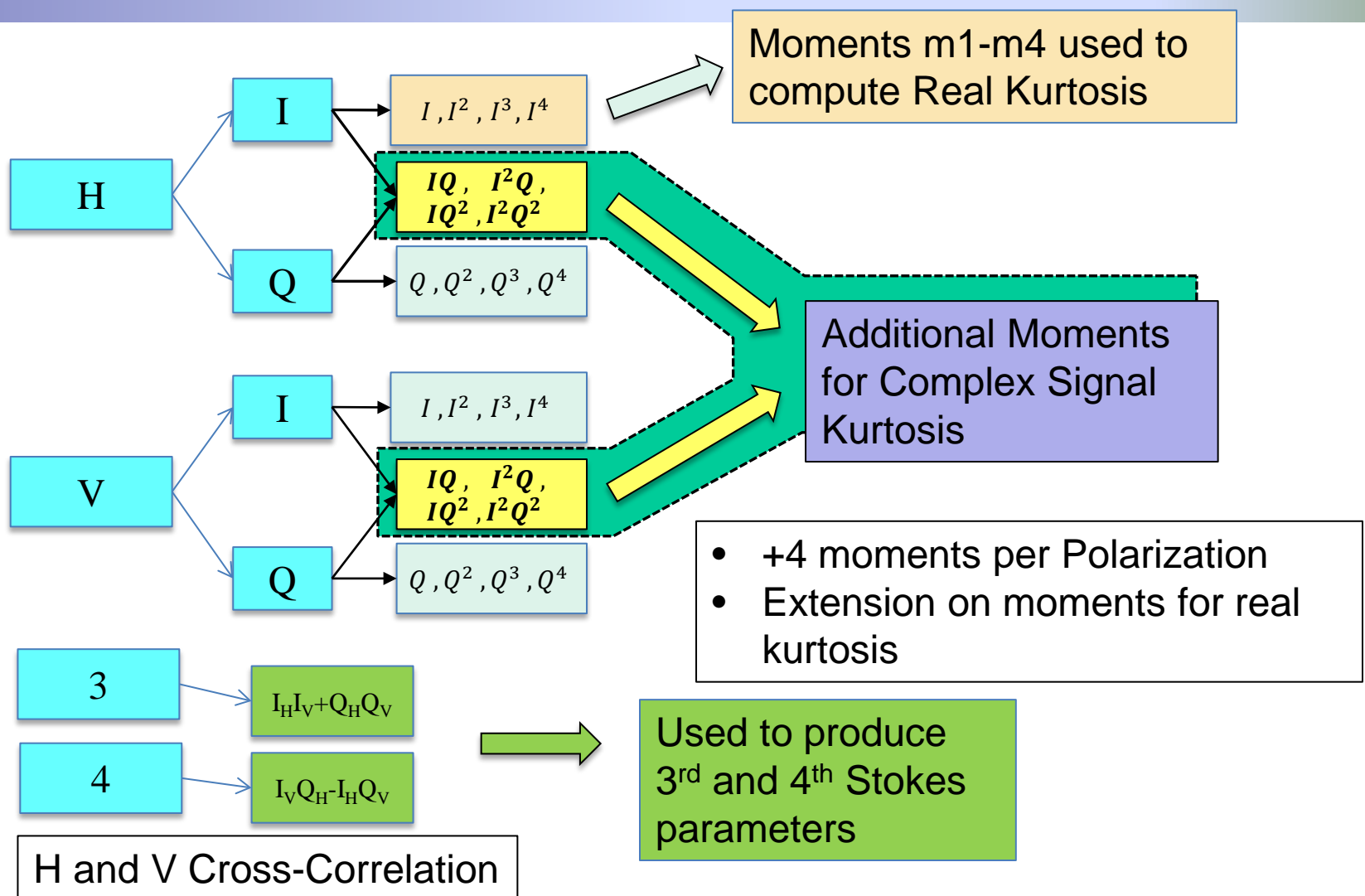
- Modules similar to these operate at 10.687 GHz designated for indoor use in the UK
- Likely offenders of GMI RFI



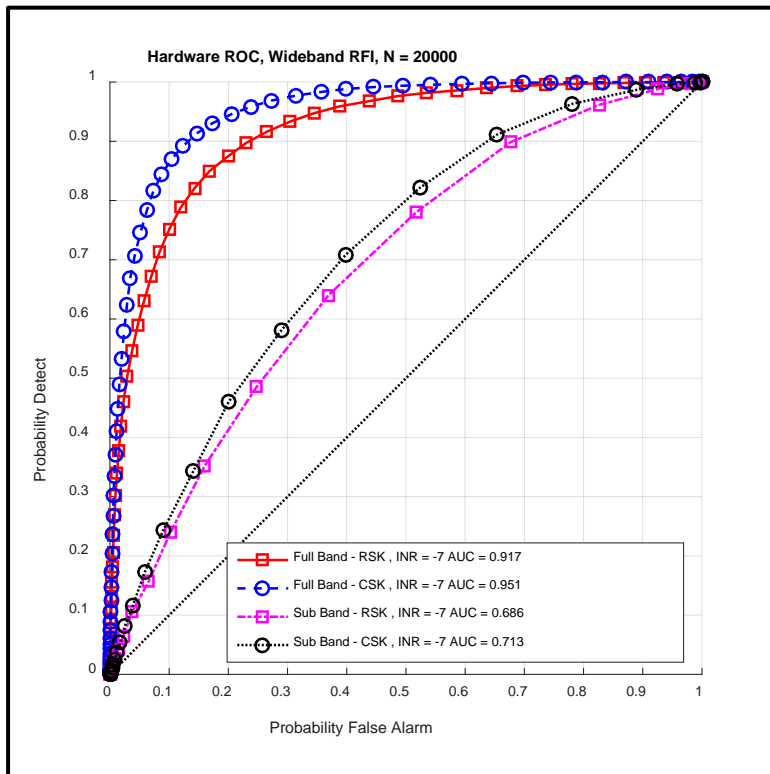
# Wideband RFI Mitigation Subsystem for Microwave Radiometers

- Technical objectives
  - Develop a wideband ( $> 200$  MHz) digital detector subsystem
  - Demonstrate innovative RFI detection and removal techniques for microwave radiometers
    - The proposed techniques are the complex values kurtosis detector and blind source separation methods. Both have the potential to improve the radio frequency interference (RFI) detection rate in high frequency bandwidth.
- 800 MHz sample-rate (200 MHz bandwidth) polarimetric radiometer test-bed was developed using the Reconfigurable Open Architecture Computing Hardware (ROACH2) system from the Collaboration for Astronomy Signal Processing and Electronics Research (CASPER) group at the University of California Berkeley
- Both the real and complex signal kurtosis algorithms were implemented in hardware and the outputs were compared to that of simulations developed in python

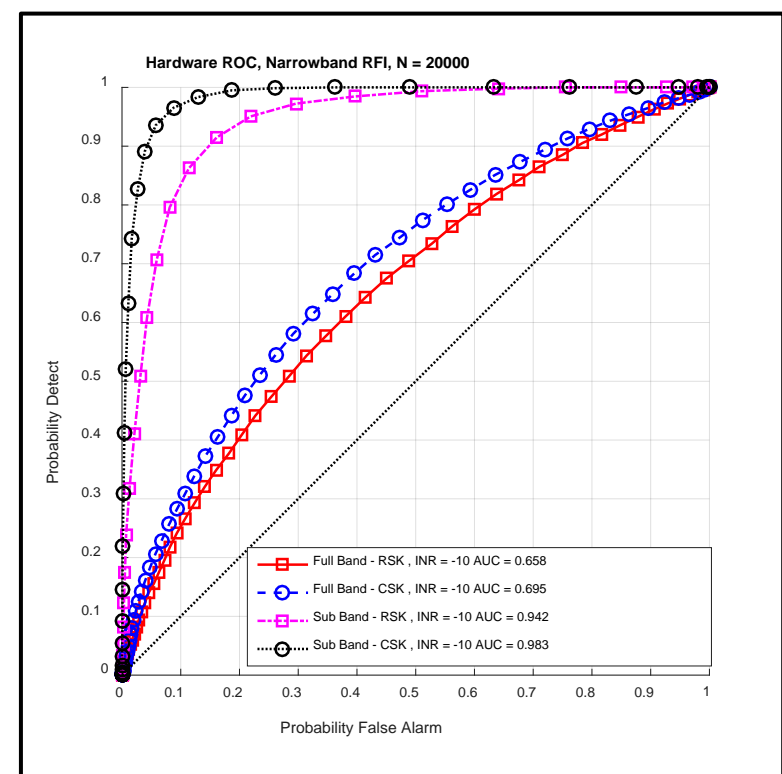
# Wideband RFI Telemetry



# Complex Kurtosis Hardware Results



QPSK signal



Narrowband CW RFI

CSK (*Complex Signal Kurtosis*) provides a better detection performance than real signal kurtosis.

Interference becomes detectable at an INR (*Interference to Noise Ratio*) of 2 dB lower than what can be detected using RSK (*Real Signal Kurtosis*).



# Blind Source Separation

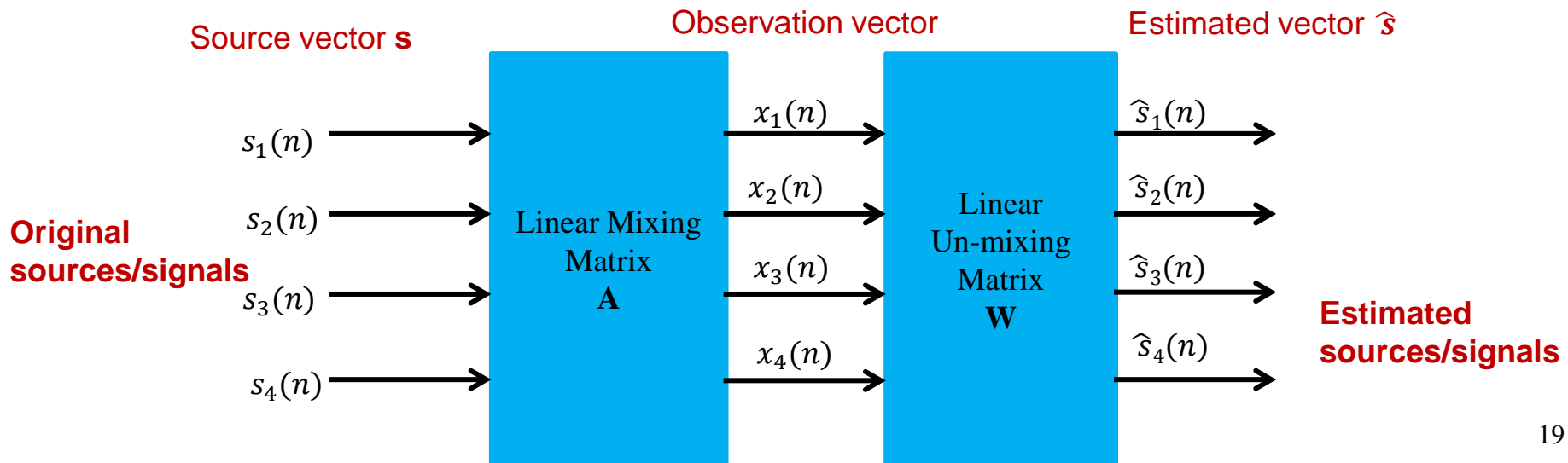
- Objective
  - Extract  $N$  unknown sources from  $P$  observations with weak assumption about sources
- Applications
  - Audio source separation, communications, ...
- Mixture Models
  - Linear instantaneous mixture
- Questions
  - Can  $\mathbf{A}$  be identified from  $\mathbf{x}(t)$  alone up to scaling of columns? (*identifiability*)
  - Can  $\mathbf{s}(t)$  be separated? (*separability*)
  - What algorithm can be used to perform these tasks?
- Ambiguity
  - Scaling
  - Permutation
- Methods
  - Independent Component Analysis:  $P \geq N$ , sources are independent
  - Sparse Component Analysis:  $P < N$ , sources have disjoint supports

$$\mathbf{x}(t) = \mathbf{A}\mathbf{s}(t), \quad t = 1, \dots, T$$

observations (known)      mixing matrix (unknown)      sources (unknown)

# Independent Component Analysis

- Can RFI be separated from noise using blind source separation; this work focuses on independent component analysis (ICA)
- Assume noise and RFI are statistically independent sources, mixing model is linear, sources are non Gaussian.
- Model:  $\mathbf{x} = \mathbf{As}$ , Observe  $\mathbf{x}$ . Sources  $\mathbf{s}$  and mixing matrix  $\mathbf{A}$  are unknown.
- $\hat{\mathbf{s}} = \mathbf{Wx}$ ,  $\hat{\mathbf{s}}$  is the estimated independent components (source estimates).



# ICA Algorithm

$$\begin{bmatrix} x_{\text{HI}}[0] & x_{\text{HI}}[1] & \dots & x_{\text{HI}}[N-1] \\ x_{\text{HQ}}[0] & x_{\text{HQ}}[1] & \dots & x_{\text{HQ}}[N-1] \\ x_{\text{VI}}[0] & x_{\text{VI}}[1] & \dots & x_{\text{VI}}[N-1] \\ x_{\text{VQ}}[0] & x_{\text{VQ}}[1] & \dots & x_{\text{VQ}}[N-1] \end{bmatrix} = \begin{bmatrix} a_{00} & a_{01} & a_{02} & a_{03} \\ a_{10} & a_{11} & a_{12} & a_{13} \\ a_{20} & a_{21} & a_{22} & a_{23} \\ a_{30} & a_{31} & a_{32} & a_{33} \end{bmatrix} \begin{bmatrix} s_{0,0} & s_{0,1} & s_{0,2} & s_{0,3} & \dots & s_{0,N-1} \\ s_{1,0} & s_{1,1} & s_{1,2} & s_{1,3} & \dots & s_{1,N-1} \\ s_{2,0} & s_{2,1} & s_{2,2} & s_{2,3} & \dots & s_{2,N-1} \\ s_{3,0} & s_{3,1} & s_{2,2} & s_{3,3} & \dots & s_{3,N-1} \end{bmatrix}$$

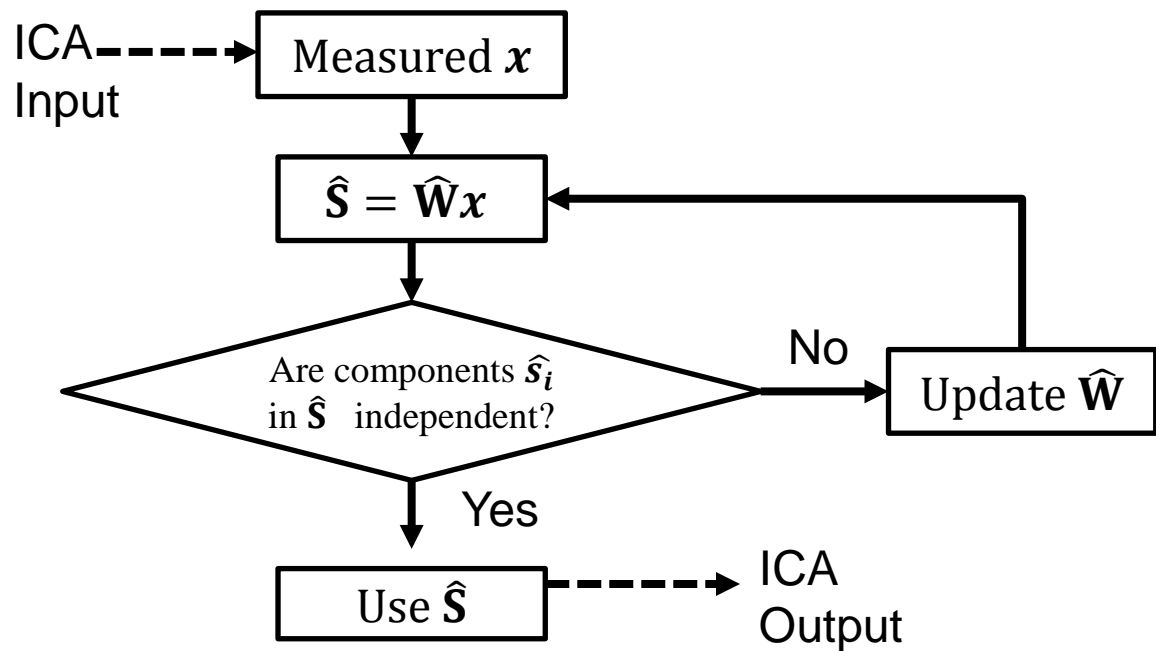
## Find A matrix to transform X into S

- Actual Signals,  $\mathbf{S}$ , are mixed by mixing matrix,  $\mathbf{A}$ , and observed as  $\mathbf{X}$
- We pick a matrix,  $\widehat{\mathbf{W}}$ , that gives us back our estimated signals,  $\widehat{\mathbf{S}}$

$$x = As$$

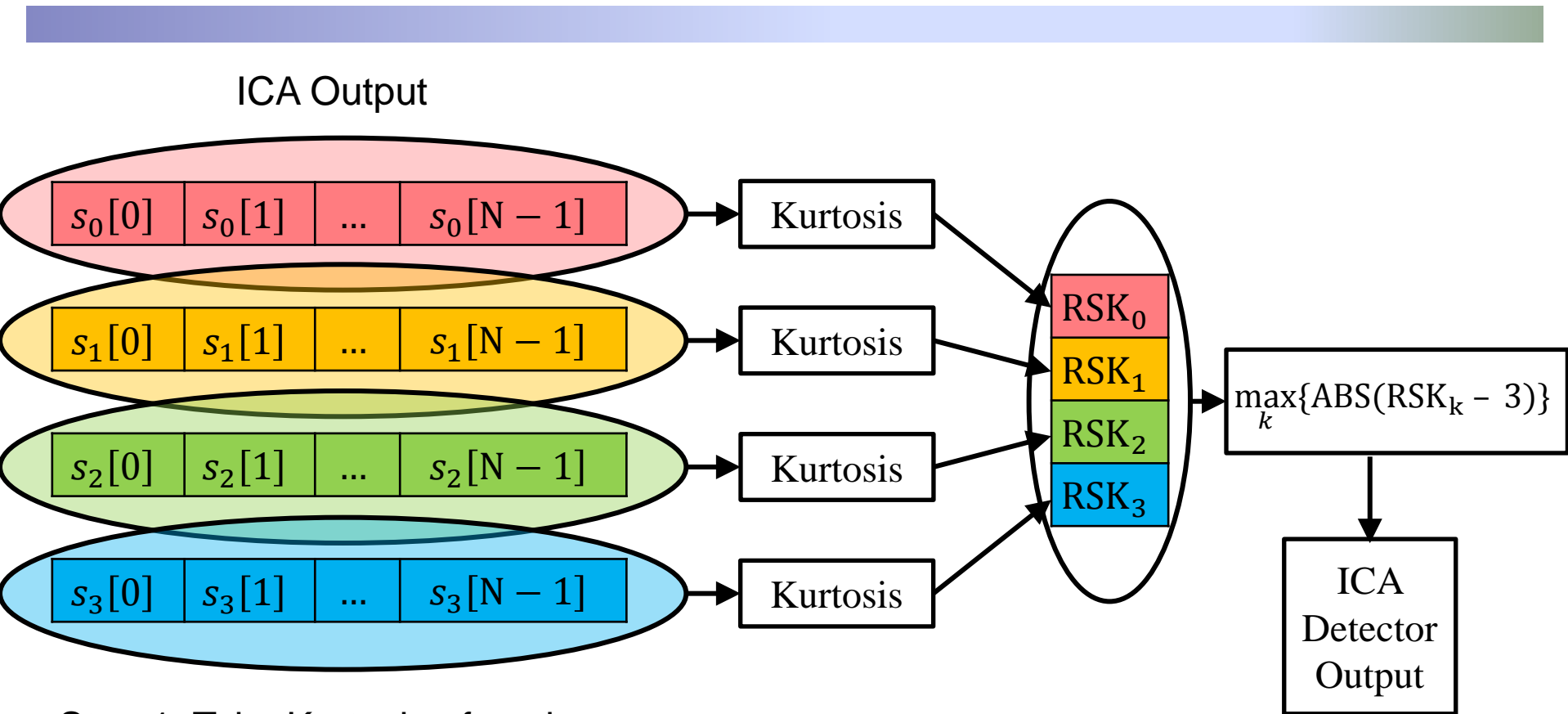
$$W = A^{-1}$$

$$\mathbf{s} = \mathbf{Wx}$$





# RFI Detection

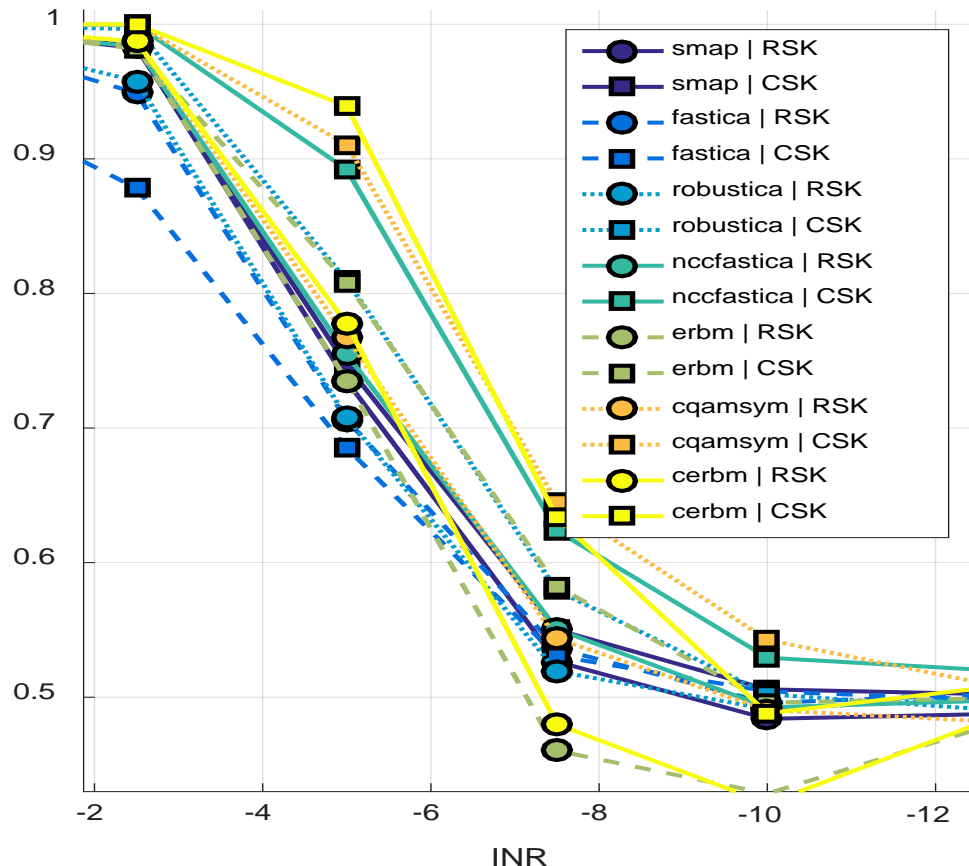


Step 1: Take Kurtosis of each estimated independent component vector

Step 2: Select the kurtosis value that deviated the furthest from 3

# AUC Results – ICA Performance – Wide Band

ICA Performance, DVBS2 , d = 100%, N = 9000

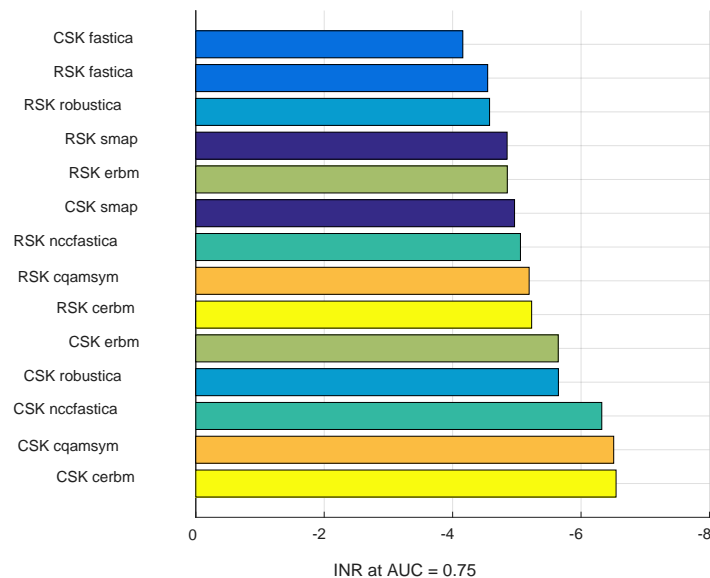


RSK = Real Signal Kurtosis

CSK = Complex Signal Kurtosis

+2dB INR Gain,  
Complex Signal Kurtosis  
with Complex ICA  
Algorithms Performs Best  
on DVB-S2

ICA Performance, DVBS2 , d = 100%, N = 9000





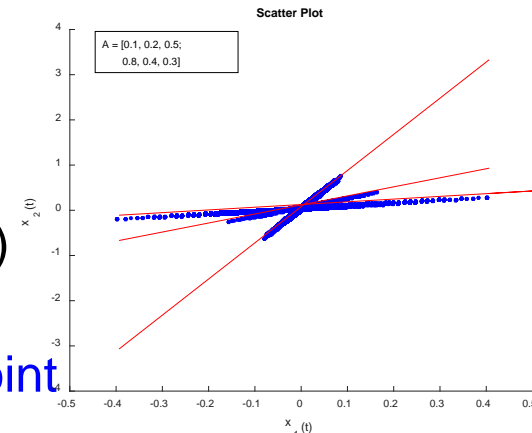
# ICA

- CSK provides better detection over RSK
- ICA assumes a critically or over determined system of independent components
- Using existing V/H polarimetric instrument architecture we are limited to two observations but there are a minimum of three independent components in the event that RFI is present
- Hence 3 or more observations are needed; current problem is therefore an under determined case for which ICA does not work well

# Sparse Component Analysis

- Application

- BSS for  $P < N$   
(under-determined)



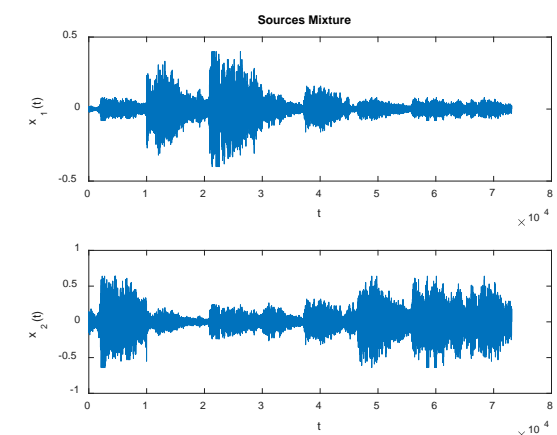
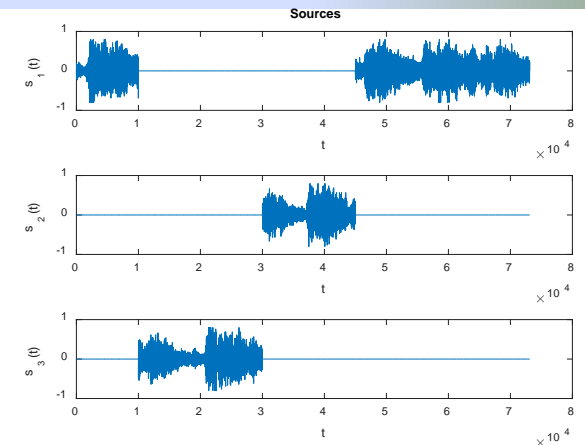
- Assumption

- Sources have disjoint supports

- Model

- $$x(t) = As(t) = [A_1, \dots, A_N] \begin{bmatrix} s_1(t) \\ \vdots \\ s_N(t) \end{bmatrix}, \quad t \in \{1, \dots, T\}$$

- $$\text{Least squares: } \hat{s}_n(t) = \begin{cases} \frac{\langle x(t), \hat{A}_n \rangle}{\|\hat{A}_n\|^2} & t \in \hat{\Lambda}_n \\ 0 & \text{otherwise} \end{cases}$$

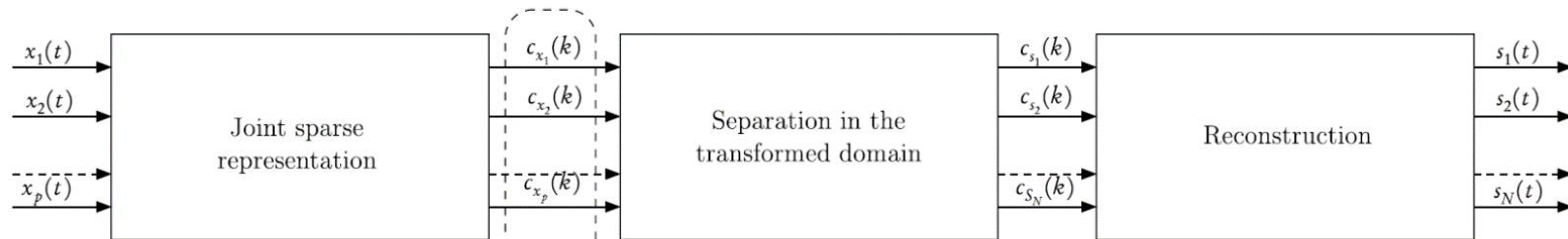




# SCA In Practice

- In practice sources are not disjoint in time!
- Method: change the representation of the observations so that in the new representation, the sources are disjoint

Mixture



## Algorithms I

- Dictionary
  - Dictionary learning
  - Structured dictionary
- Joint sparse representation
  - Global optimization
  - Greedy algorithm
- Mixing matrix estimation
  - Global clustering
  - Local scatter plots
- Separation
  - Binary masking

## Algorithms II

- Dictionary
  - **Structured dictionary- different set of dictionaries**
- Joint sparse representation
  - **Global optimization- exact sparse coding**
- Mixing matrix estimation
  - Global clustering – Weighted histogram
- Separation
  - **Local separation**

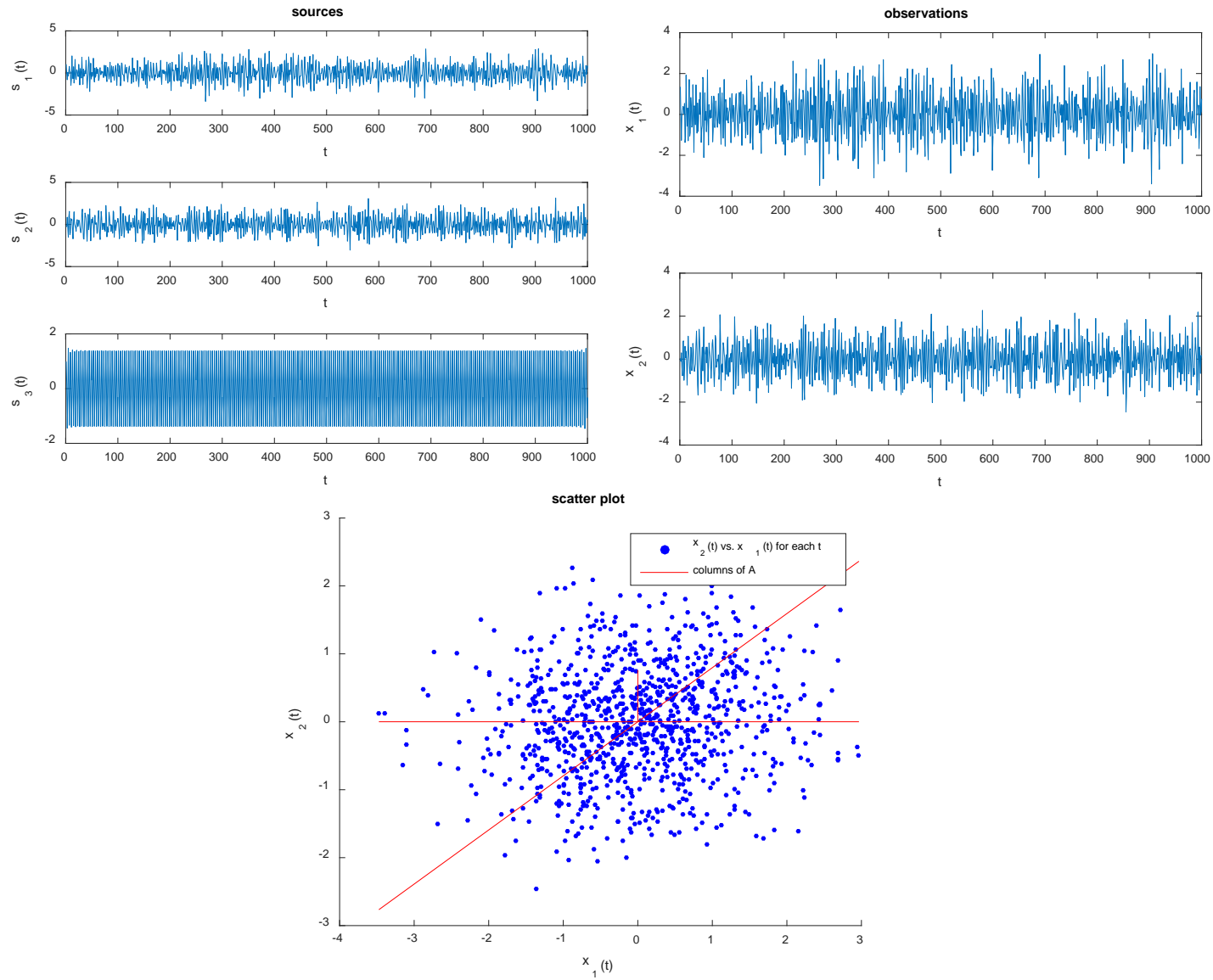


# Sparse Signal Representation

- Satisfying the SCA Assumption
  - Represent each source by a linear combination of a few elementary signals (**atoms**):  $s(t) = \sum_{k=1}^K c_s(k)\varphi_k(t)$
- Measure of sparsity
  - $\|c_s\|_\tau = \begin{cases} \left(\sum_{k=1}^K |c_s(k)|^\tau\right)^{1/\tau} & \tau > 0 \\ \text{num of nonzero coefficients} & \tau = 0 \end{cases}$  quantifies the sparsity of  $c_s$
  - Ideal  $\tau$  for sparsity is 0
- Dictionary
  - **Dictionary**: set of atoms
  - Consider dictionaries that span  $C^T$ 
    - $K > T$ : **redundant dictionary**, infinite representation
- Synthesis
  - $s = c_s \Phi$
- Effective Dictionary: enables a sparse representation

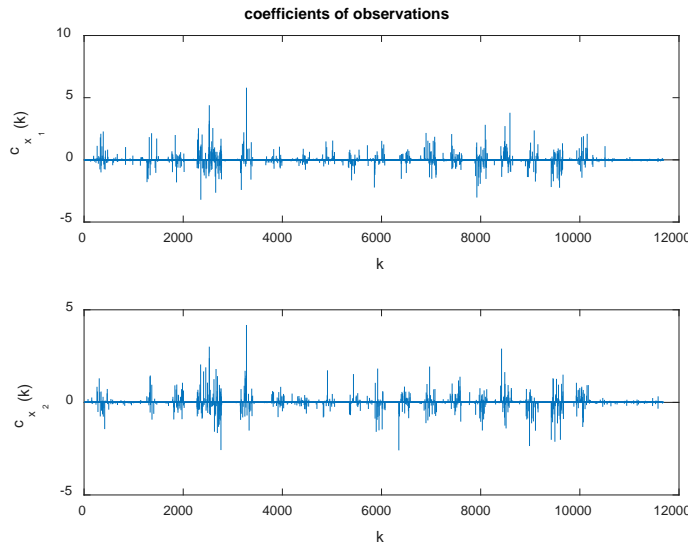


# SCA Example: Sources with non disjoint supports

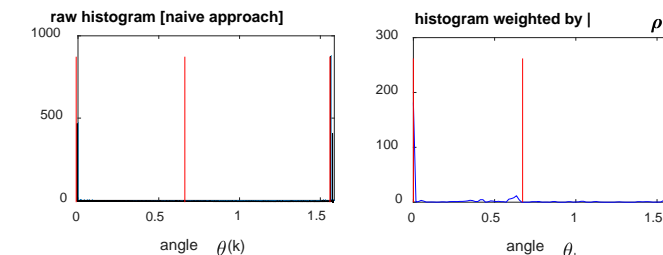
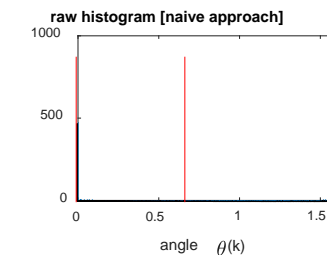
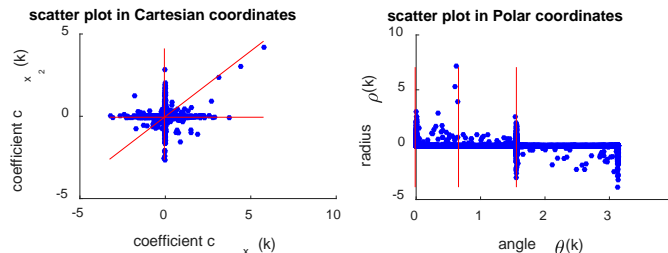
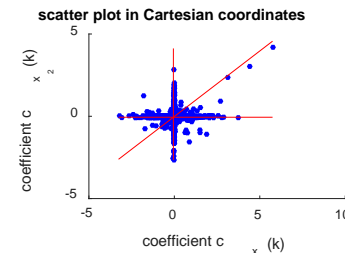




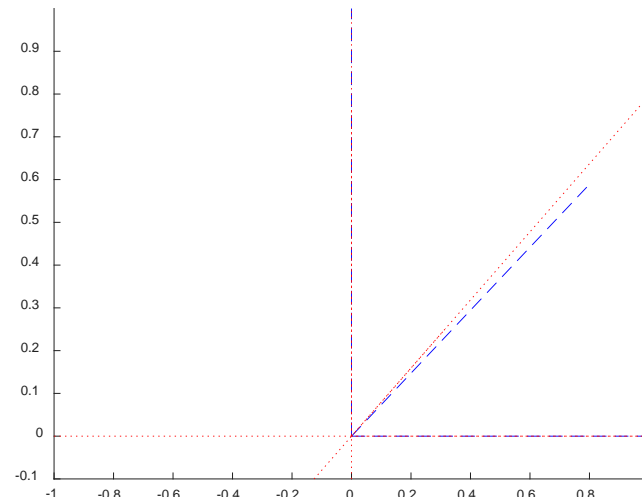
# Sparse Representation and Estimating Mixing Matrix



Sparse  
Representation

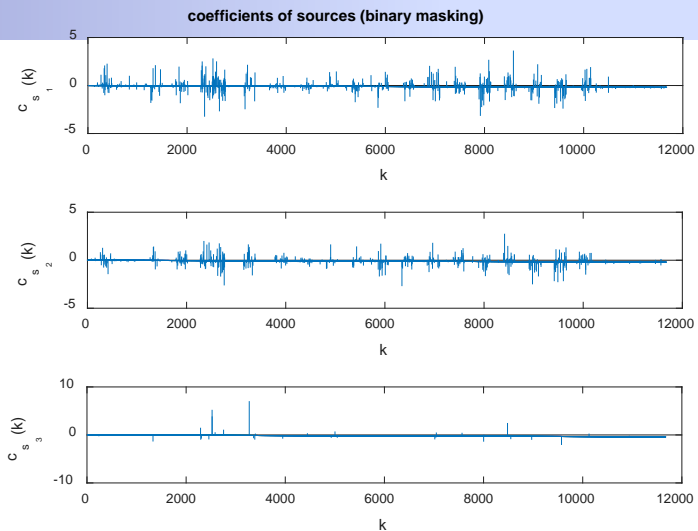


Estimating  
Mixing Matrix

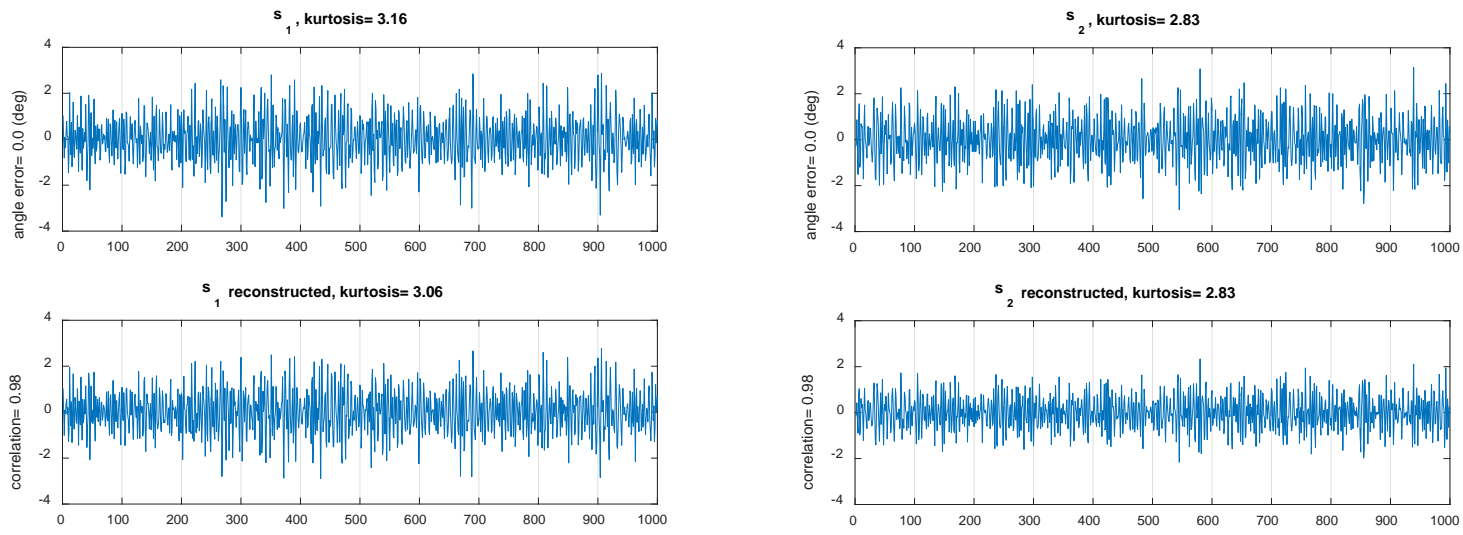


# Separation and Reconstruction

## Separation



## Reconstruction





# Simulation Results – Estimating Noise

Measure of performance: correlation between original noise and reconstructed noise

		$E[ \text{corr. coeff. btw } n_H \text{ and } \hat{n}_H ]$	$E[ \text{corr. coeff. btw } n_V \text{ and } \hat{n}_V ]$	INR (dB)				
		Greedy Algorithm		no RFI	-25	-20	-15	-10
duty-cycle	100%	0.985, 0.979			0.982, 0.977	0.978, 0.975	0.972, 0.970	0.965, 0.958
	1%				0.983, 0.978	0.978, 0.975	0.970, 0.966	0.953, 0.946

		INR (dB)					
		no RFI	-25	-20	-15	-10	
		Global Optimization	0.988, 0.986	0.987, 0.981	0.984, 0.981	0.981, 0.974	0.977, 0.973
duty-cycle	100%	0.987, 0.986		0.987, 0.981	0.984, 0.980	0.976, 0.970	0.961, 0.949
	1%						



# Simulation Results – Estimating Noise Power

- Requires scale estimation
  - Scale =  $\text{median}(\text{reconstructed noise} / \text{original noise})$
  - In practice, scale can be estimated by exploiting neighbors scale
- Measure of performance: relative error between power of reconstructed noise and power of original noise

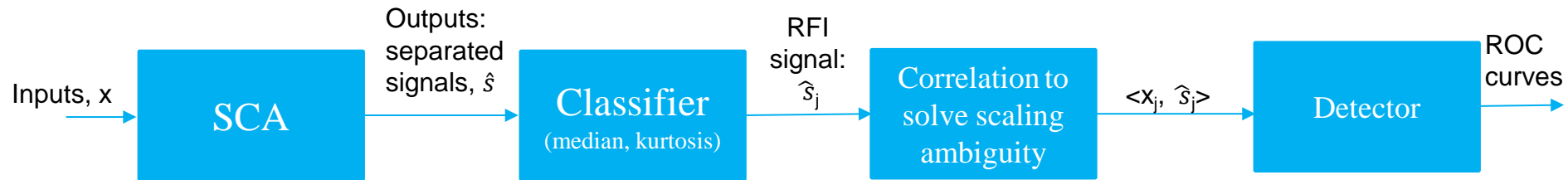
$$E \left[ \frac{\text{var}(\text{scl}_H * \widehat{n}_H) - \text{var}(n_H)}{\text{var}(n_H)} \right] \times 100\%$$

$$E \left[ \frac{\text{var}(\text{scl}_V * \widehat{n}_V) - \text{var}(n_V)}{\text{var}(n_V)} \right] \times 100\%$$

		INR (dB)				
<u>Greedy Algorithm</u>		no RFI	-25	-20	-15	-10
duty-cycle	100%		4.7, 4.5	3.2, 4.0	5.9, 5.7	6.1, 6.5
	1%	1.9, 2.5	2.3, 3.5	3.1, 3.9	4.8, 5.5	8.2, 10.0

		INR (dB)				
<u>Global Optimization</u>		no RFI	-25	-20	-15	-10
duty-cycle	100%		1.1, 1.7	1.9, 4.1	3.5, 7.8	4.9, 6.7
	1%	0.6, 2.6	0.9, 5.2	1.6, 4.2	2.8, 5.9	6.0, 8.8

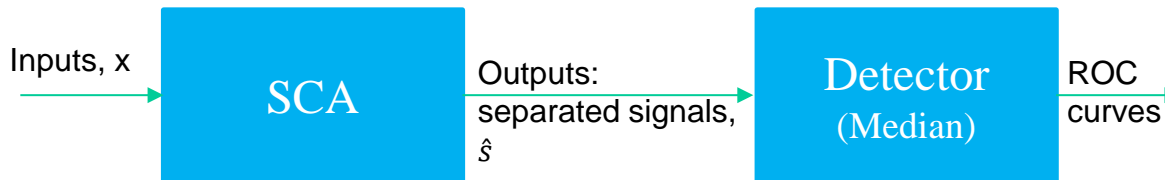
# RFI Detection



- SCA scaling ambiguity is evident from previous simulations
  - Use correlation after classification to minimize scaling ambiguity
- Use statistical measures as classifiers
- Use statistical measures such as median, kurtosis, etc. as detectors
  - Pass only predicted RFI signal through detector

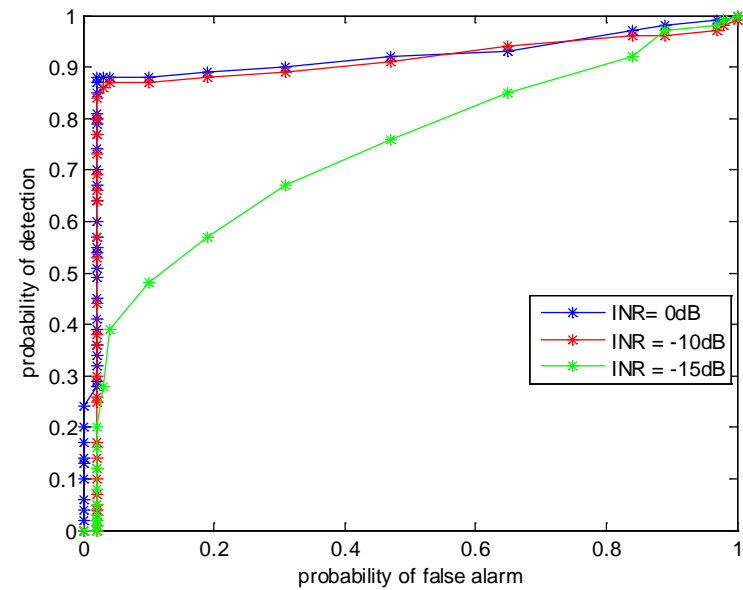
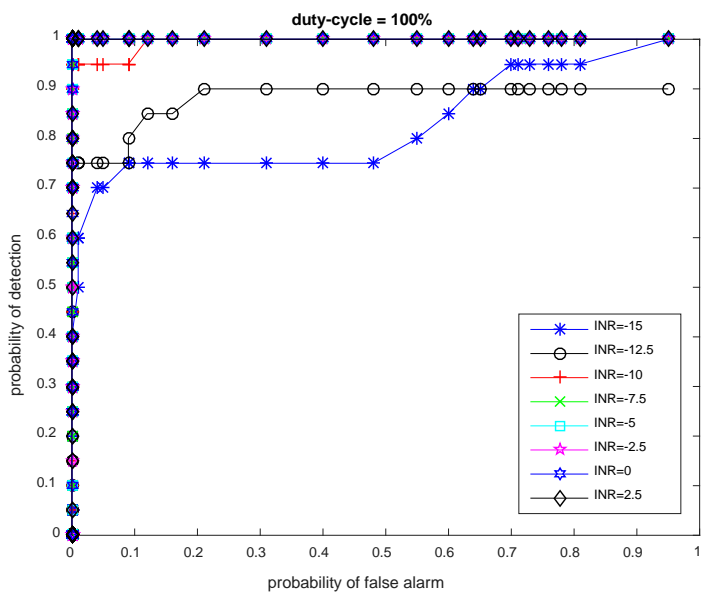
# RFI Detection Using SCA

- Detection criteria:  $\text{median}(\text{abs}(\text{reconstructed sources}))$
- SCA is capable of detecting RFI with high INR and high duty-cycle



- **Detector:**
  - Prob. Detection:
    - Median of absolute value of reconstructed sources **H1** > threshold
  - Prob. False Alarm:
    - Median of absolute value of reconstructed sources **H0** > threshold
- ROC thresholds: 0:0.01:1

# RFI Detection By Median



## Algorithms I

- Dictionary
  - Structured dictionary
- Joint sparse representation
  - Greedy algorithm - OMP
- Mixing matrix estimation
  - Global clustering – Weighted histogram
- Separation
  - Binary masking

## Algorithms II

- Dictionary
  - **Structured dictionary- different set of dictionaries**
- Joint sparse representation
  - **Global optimization- exact sparse coding**
- Mixing matrix estimation
  - Global clustering – Weighted histogram
- Separation
  - **Local separation**



# Conclusions

- SMAP's current algorithms for RFI detection and mitigation are performing well
- Sources that are wideband and occupy much of the bandwidth cannot be corrected by any of SMAP's RFI filtering algorithms
- Blind source separation results indicate that these type of algorithms are not sensitive enough for the RFI detection problem and they are also quite computationally intensive
- These results indicate the need for continued protection of spectrum



# ICA Algorithms

- **Fast ICA (FASTICA)**
  - A. Hyvärinen. "Fast and Robust Fixed-Point Algorithms for Independent Component Analysis", *IEEE Transactions on Neural Networks* 10(3):626-634, 1999.
- **Robust ICA (ROBUSTICA)**
  - V. Zarzoso and P. Comon, "Robust Independent Component Analysis by Iterative Maximization of the Kurtosis Contrast with Algebraic Optimal Step Size", *IEEE Transactions on Neural Networks*, Vol. 21, No. 2, February 2010, pp. 248-261.
- **Non Circular Complex Fast ICA (NCCFASTICA)**
  - Mike Novey and T. Adali, "On Extending the complex FastICA algorithm to noncircular sources" *IEEE Trans. Signal Processing*, vol. 56, no. 5, pp. 2148-2154, May 2008.
- **Entropy Rate Bound Minimization (ERBM)**
  - X.-L. Li, and T. Adali, "Blind spatiotemporal separation of second and/or higher-order correlated sources by entropy rate minimization," in *Proc. IEEE Int. Conf. Acoust., Speech, Signal Processing (ICASSP)*, Dallas, TX, March 2010.
- **Complex Quadrature Amplitude Modulation (CQAMSYM)**
  - Mike Novey and T. Adali, "Complex Fixed-Point ICA Algorithm for Separation of QAM Sources using Gaussian Mixture Model" in *IEEE Conf. ICASSP 2007*
- **Complex Entropy Rate Bound Minimization (CERBM)**
  - G.-S. Fu, R. Phlypo, M. Anderson, and T. Adali, "Complex Independent Component Analysis Using Three Types of Diversity: Non-Gaussianity, Nonwhiteness, and Noncircularity," *IEEE Trans. Signal Processing*, vol. 63, no. 3, pp. 794-805, Feb. 2015.